LETTERS

An asymmetric explosion as the origin of spectral evolution diversity in type Ia supernovae

K. Maeda[1], S. Benetti[2], M. Stritzinger[3,4], F. K. Röpke[5], G. Folatelli[6], J. Sollerman[4,7], S. Taubenberger[5], K. Nomoto[1], G. Leloudas[4], M. Hamuy[6], M. Tanaka[1], P. A. Mazzali[5,8] & N. Elias-Rosa[9]

Type Ia supernovae form an observationally uniform class of stellar explosions, in that more luminous objects have smaller decline-rates[1]. This one-parameter behaviour allows type Ia supernovae to be calibrated as cosmological 'standard candles', and led to the discovery of an accelerating Universe[2,3]. Recent investigations, however, have revealed that the true nature of type Ia supernovae is more complicated. Theoretically, it has been suggested[4–8] that the initial thermonuclear sparks are ignited at an offset from the centre of the white-dwarf progenitor, possibly as a result of convection before the explosion[4]. Observationally, the diversity seen in the spectral evolution of type Ia supernovae beyond the luminosity–decline-rate relation is an unresolved issue[9,10]. Here we report that the spectral diversity is a consequence of random directions from which an asymmetric explosion is viewed. Our findings suggest that the spectral evolution diversity is no longer a concern when using type Ia supernovae as cosmological standard candles. Furthermore, this indicates that ignition at an offset from the centre is a generic feature of type Ia supernovae.

When a carbon-oxygen white dwarf reaches a critical limit known as the Chandrasekhar mass (~1.38 solar masses), its central density and temperature increase to a point where a thermonuclear runaway is initiated. The thermonuclear sparks give birth to a subsonic deflagration flame, which at some point may make a transition to a supersonic detonation wave that leads to the complete disruption of the white dwarf[11,12]. The thermalization of γ-rays produced from the decay of freshly synthesized radioactive ^{56}Ni powers the transient source, known as a type Ia supernova[13,14]. The relationship between the luminosity and the decline-rate parameter (Δm_{15}(B), which is the difference between the B-band magnitude at peak and that measured 15 days later) is interpreted to be linked to the amount of newly synthesized ^{56}Ni (refs 15, 16).

Type Ia supernovae displaying a nearly identical photometric evolution can exhibit appreciably different expansion velocity gradients ($\dot{v}_{\rm Si}$), as inferred from the Si II 6,355 Å absorption feature[10,17]. More specifically, objects that show $\dot{v}_{\rm Si} \gtrsim 70$ km s^{-1} d^{-1} are placed into the high-velocity gradient (HVG) group, while those that show smaller gradients are placed in the low-velocity gradient (LVG) group. For normal type Ia supernovae[18], which are the predominant population of the total type Ia supernova sample and the main focus of this Letter, $\dot{v}_{\rm Si}$ is not correlated with $\Delta m_{15}(B)$ (ref. 10; Fig. 1a, b), thus raising a nagging concern regarding the 'one-parameter' description.

Late phase nebular spectra can be used to trace the distribution of the inner ejecta[19]. Beginning roughly half a year after explosion, as the ejecta expands, its density decreases to the point where photons freely escape. Photons originating from the near/far side of the ejecta are detected at a shorter/longer (blue-shifted/red-shifted) wavelength because of Doppler shifts. For type Ia supernovae, emission lines related to [Fe II] 7,155 Å and [Ni II] 7,378 Å are particularly useful, as they are formed in the ashes of the deflagration flame[19]. These lines show diversity in their central wavelengths—blue-shifted in some type Ia supernovae and red-shifted in others (see Fig. 1c)—which provides evidence that the deflagration ashes, therefore the initial sparks, are on average located off-centre. The wavelength shift can be translated to a line-of-sight velocity ($v_{\rm neb}$) of the deflagration ashes.

Figure 2 shows a comparison between $\dot{v}_{\rm Si}$ and $v_{\rm neb}$ for 20 type Ia supernovae. Details regarding the data are provided in Supplementary Information section 1. Although the diversities in these observables were discovered independently, Fig. 2 clearly shows that they are connected. Omitting the peculiar SN 2004dt (Fig. 2 legend; Supplementary Information section 1), all 6 HVG supernovae show $v_{\rm neb} > 0$ km s^{-1} (that is, red-shifts), which means that these events are viewed from the direction opposite to the off-centre initial sparks. The 11 LVGs display a wider distribution in $v_{\rm neb}$ space, but are concentrated to negative values (that is, blue-shifted), indicating that these events are preferentially viewed from the direction of the initial sparks. If HVG and LVG supernovae were intrinsically distributed homogeneously as a function of $v_{\rm neb}$, the probability that just by chance (as a statistical fluctuation) all HVG supernovae show $v_{\rm neb} > 0$ km s^{-1} is merely 0.4%; it is thus quite unlikely. Indeed, the probability that by chance six HVG supernovae are among the seven supernovae showing the largest red-shift in $v_{\rm neb}$ in our sample of 17 supernovae is only 0.06%.

This finding strongly indicates that HVG and LVG supernovae do not have intrinsic differences, but that this diversity arises solely from a viewing angle effect. Figure 3 shows a schematic picture. If viewed from the direction of the off-centre initial sparks, a type Ia supernova appears as an LVG event at early phases and shows blue-shifts in the late-time emission lines. If viewed from the opposite direction, it appears as an HVG event, and shows red-shifts at late phases.

The number of HVG supernovae is ~35% of the total number of HVG and LVG supenovae[10]. To explain this, the angle to the observer at which a supernova changes its appearance from an LVG to an HVG is ~105–110°, measured relative to the direction between the centre and the initial spark. The velocity shift of 3,500 km s^{-1} in the distribution of the deflagration ashes, as derived for the normal type Ia SN 2003hv through a detailed spectral analysis[19], corresponds to $v_{\rm neb} \approx 1{,}000$ km s^{-1} if viewed from this transition angle. The configuration then predicts that all LVG supernovae should show

[1]Institute for the Physics and Mathematics of the Universe (IPMU), University of Tokyo, 5-1-5 Kashiwanoha, Kashiwa, Chiba 277-8583, Japan. [2]INAF — Osservatorio Astronomico di Padova, vicolo dell'Osservatorio 5, I-35122 Padova, Italy. [3]Carnegie Institute for Science, Las Campanas Observatory, Colina el Pino Casilla 601, La Serena, Chile. [4]Dark Cosmology Centre, Niels Bohr Institute, Copenhagen University, Juliane Maries Vej 30, 2100 Copenhagen Ø, Denmark. [5]Max-Planck-Institut für Astrophysik, Karl-Schwarzschild-Straße 1, 85741 Garching, Germany. [6]Universidad de Chile, Departamento de Astronomía, Casilla 36-D, Santiago, Chile. [7]The Oskar Klein Centre, Department of Astronomy, Stockholm University, AlbaNova, 10691 Stockholm, Sweden. [8]Scuola Normale Superiore, Piazza Cavalieri 7, 56127 Pisa, Italy. [9]Spitzer Science Center, California Institute of Technology, 1200 E. California Blvd, Pasadena, California 91125, USA.

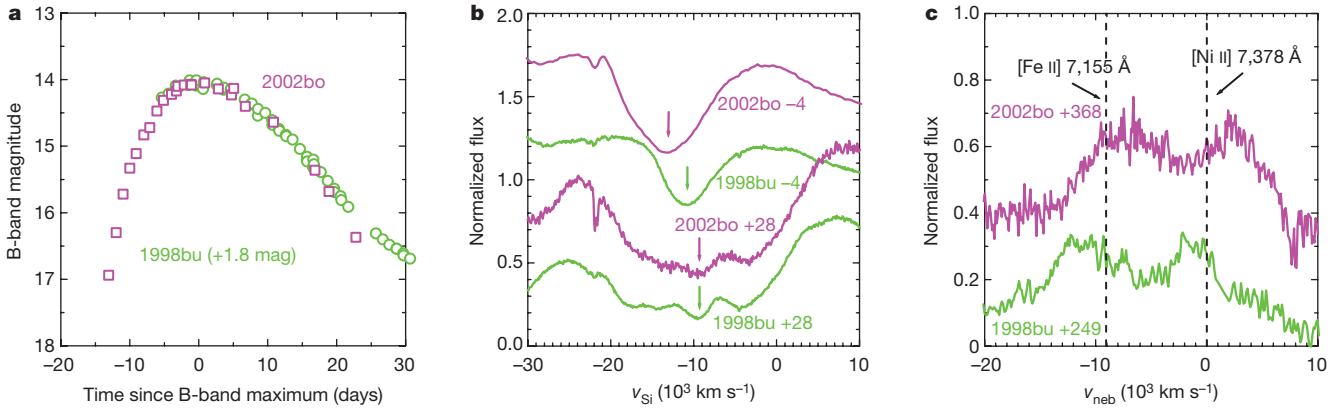

Figure 1 | Comparison between HVG type Ia SN 2002bo and LVG type Ia SN 1998bu. The decline-rate parameter $\Delta m_{15}(B)$ is 1.16 mag and 1.06 mag for SN 2002bo and SN 1998bu, respectively. **a**, The B-band light curves[17,24]. The magnitudes for SN 1998bu have been artificially shifted in the *y*-direction for presentation. **b**, Si II 6,355 Å at different epochs[17,24] (in days with respect to B-band maximum). SN 2002bo had initially a larger absorption velocity than SN 1998bu, but later its velocity approached that of SN 1998bu. The velocity evolved quicker and the velocity gradient ($\dot{v}_{Si}$) is larger for SN 2002bo than for SN 1998bu. **c**, [Fe II] 7,155 Å and [Ni II] 7,378 Å in late-time spectra[21,25]. The horizontal axis denotes the line velocity measured from the rest wavelength of [Ni II] 7,378 Å. The rest wavelengths of [Fe II] 7,155 Å and [Ni II] 7,378 Å are marked by dashed lines. These lines are red-shifted in SN 2002bo while being blue-shifted in SN 1998bu. The wavelength shift indicates the line-of-sight velocity of the deflagration ashes (v_{neb}) ($v_{neb} < 0$ km s^{-1}, that is, the blue-shift, if the material is moving towards us). These are the strongest lines among those emitted from the deflagration ash according to the previous analysis of late-time emission lines[19]. Indeed, there are stronger lines which do not show Doppler shifts, for example, [Fe III] 4,701 Å; they however do not trace the distribution of the deflagration ash[19] (see also Supplementary Information section 1) and are thus not useful in the present study.

$-3{,}500 < v_{neb} < 1{,}000$ km s^{-1}, while all HVG supernovae should be in the range $1{,}000 < v_{neb} < 3{,}500$ km s^{-1}. These ranges are shown as arrows in Fig. 2, and provide a good match to the observations.

Figure 4a shows an example of a hydrodynamic model in which the thermonuclear sparks were ignited off-centre in a Chandrasekhar-mass white dwarf[6] (an alternative way of introducing global asymmetries is double detonations in sub-Chandrasekhar-mass white dwarfs[20]). Although this model has not been fine-tuned to reproduce the present finding, it does have the required generic features. The density distribution is shallow and extends to high velocity in the direction opposite to the initial sparks (Fig. 4b). Initially, the photosphere is at high velocity if viewed from this direction, as the region at the outer, highest velocities is still opaque. Later on, the photosphere recedes inwards faster in this opposite direction, owing to the shallower density gradient. As a result, the supernova looks like an LVG if viewed from the offset direction, but like an HVG supernova from the opposite direction (Fig. 4c), as in our proposed picture (Fig. 3).

Our finding provides not only strong support for the asymmetric explosion as a generic feature, but also constraints on the still-debated deflagration-to-detonation transition. In this particular simulation, the change in appearance (as an HVG or an LVG supernova) takes place rather abruptly around the viewing direction of ~140°. Owing to the offset ignition, the deflagration flame propagates asymmetrically and forms an off-centre, shell-like region of high-density deflagration ash. The detonation is ignited at an offset following the deflagration, but tries to expand almost isotropically. However, the angle between 0° and 140° is covered by the deflagration ash, into which the strong detonation wave (fuelled by the unburned material near the centre of the white dwarf) cannot penetrate. On the other hand, in the 140–180° direction, the detonation can expand freely, creating a shallow density distribution. The 'abrupt' change in appearance, as inferred by the observational data, is therefore a direct consequence of the offset models, controlled by the distribution of the deflagration ash. The 'opening angle' of the

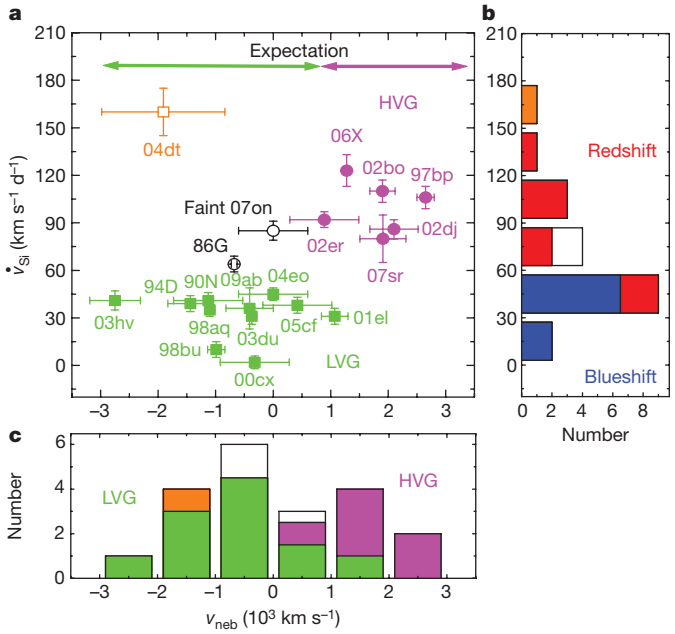

Figure 2 | Relations between the features in early and late phases. a, Early-phase velocity gradient ($\dot{v}_{Si}$, vertical axis) as compared to late-phase emission-line shift velocity (v_{neb}, horizontal axis) for 20 type Ia supernovae. The errors are for 1σ in fitting the velocity evolution for $\dot{v}_{Si}$, while for v_{neb} the errors are from differences in measurement between different emission lines (see Supplementary Information section 1). LVG supernovae and HVG supernovae are shown by green squares and magenta circles, respectively. SN 1986G and SN 2007on are classified as 'faint and fast-declining' type Ia supernovae[26–28] (black open circles). SN 2004dt (orange square) is an HVG supernova according to the value of $\dot{v}_{Si}$, but displayed peculiarities in the late-time spectrum[29] (Supplementary Information section 1) and in polarization measurements[22] (Supplementary Information section 2), and the value for $\dot{v}_{Si}$ is exceptionally large compared to other HVG supernovae. These suggest that SN 2004dt is an outlier, and the origin of its large $\dot{v}_{Si}$ is probably different from that of other type Ia supernovae. The two arrows on top indicate the regions where HVG and LVG supernovae are expected, based on a simple kinematic interpretation (see main text). **b**, Number distribution of 20 supernovae as a function of $\dot{v}_{Si}$. White and orange areas are for faint supernovae and SN 2004dt. The remaining supernovae are marked depending on whether they show a blue-shift ($v_{neb} < 0$ km s^{-1}: blue area) or red-shift ($v_{neb} > 0$ km s^{-1}: red area) in their late-time spectra. **c**, Number distribution of 20 supernovae as a function of v_{neb}.

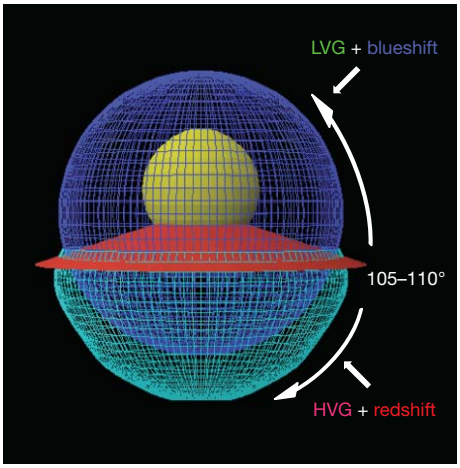

Figure 3 | A schematic picture of the structure of type Ia supernovae ejecta. This configuration simultaneously explains the relative fractions of HVG and LVG type Ia supernovae, and the relation between $\dot{v}_{Si}$ and v_{neb}. It is also consistent with the diversity in v_{neb} (ref. 19). The ashes of the initial deflagration sparks are shifted with respect to the centre of the supernova ejecta by ~3,500 km s^{-1} (yellow: although expressed by a spherical region for presentation, it may well have an amorphous shape owing to the hydrodynamic instability in the deflagration flame[7]). This region is rich in stable ^{58}Ni with a small amount of radioactive ^{56}Ni, and emits [Fe II] 7,155 Å and [Ni II] 7,378 Å at late phases[19] (Supplementary Information section 1). The outer region is the later detonation ash responsible for the early-phase Si II 6,355 Å absorption. This region is roughly spherically distributed (blue), but extends to the outer region in the direction opposite to the deflagration ashes (cyan). Although the detonation can produce ^{56}Ni, which decays into ^{56}Fe, it has been argued that these regions (blue and cyan) are not main contributors to [Fe II] 7,155 Å and [Ni II] 7,378 Å at late phases[19] (Supplementary Information section 1). A putative observer would view this explosion as an LVG or HVG supernova, depending on the direction of the observer, as divided by a specific angle (red), which is ~105–110°. This angle is derived from the relative numbers of HVG and LVG supernovae (see main text); the fraction of HVG supernovae to the total number of HVG and LVG supernovae ~35% (ref. 10), as was also supported by a larger sample[30] with more than 100 supernovae (using the observed trend that the HVG supernovae show higher velocities than LVG objects at early times).

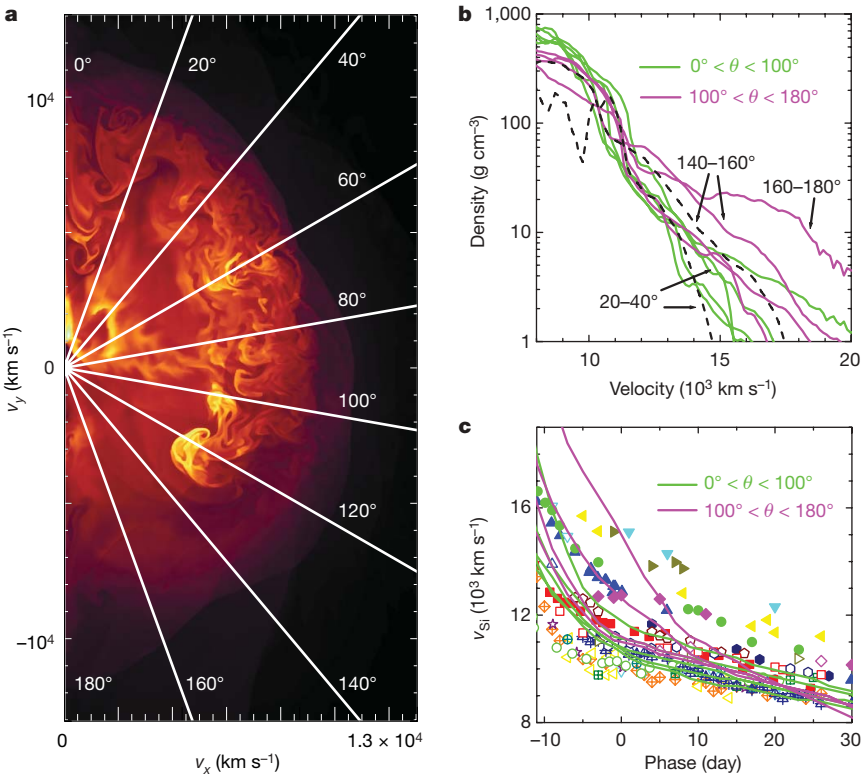

Figure 4 | Expectations from a hydrodynamic explosion model. a, Cross-section of the density distribution of an offset ignition model[6] (similar to a model in ref. 5). It is shown at 10 s after the ignition, when the homologous expansion is already reached. In this model, the deflagration sparks were ignited at an offset, within an opening angle of 45° and within 0–180 km from the centre of a white dwarf whose radius is ~ 2,000 km. The deflagration products are distributed in the high-density offset shell, which covers 0–140° in this particular model. This resulting velocity shift is ~ 8,000 km s^{-1} in this model, which is larger than the observational requirement (~3,500 km s^{-1}). **b**, Radial density distribution of the same model for several directions (where the angle is measured from the direction of the offset sparks). The magenta lines show the density distribution for the angle in 100–180°, roughly corresponding to the putative directions for which a supernova looks like an HVG supernova inferred from the observational data (Fig. 3). Also shown is the density distribution multiplied by the mass fraction of intermediate mass elements, which gives a rough distribution of Si, for two directions (20–40° and 140–160°). It is seen that the distribution of Si roughly follows the density distribution. **c**, Model photospheric velocity evolution for several directions (lines) as compared to the observed Si II 6,355 Å absorption line evolution[10] (filled and open symbols for HVG and LVG supernovae, respectively; the phase in days with respect to B-band maximum). The position of the photosphere is estimated by integrating the optical depth with a constant opacity along each direction. Using the Si distribution for the velocity estimate provides a similar result.

transition is on the other hand dependent on the details of the explosion. To accurately model this according to our finding ($\sim$105–110° for the typical transition angle), either a smaller offset of the initial deflagration sparks or an earlier deflagration-to-detonation transition would be necessary. Such changes are also required to produce the typical velocity shift of $\sim$3,500 km s^{-1} in the distribution of the deflagration ash.

Our proposed model unifies into a single scheme recent advances in both theoretical and observational studies of type Ia supernovae—and it does not conflict with other results produced by spectral tomography[16,21] or polarization measurements[22] (Supplementary Information section 2). Our interpretation suggests that two supernovae with very similar light curve evolution may not necessarily produce exactly the same amount of ^{56}Ni. They might in fact show somewhat different light curve evolution if viewed from the same direction (relative to the offset between the centre and the initial spark) but the light curves look the same to an observer as $\Delta m_{15}(B)$ can change with viewing direction[5] (Supplementary Information section 3). This situation is a natural consequence of observing a number of type Ia supernovae with a large variation in ^{56}Ni production and in the viewing angles. Our finding regarding the explosion mechanism will lead to quantitative evaluation of the contribution of this random effect to the observed scatter in the type Ia supernova luminosities beyond the one-parameter description[5], as compared to other systematic effects, such as the stellar environment[23].

Received 12 March; accepted 20 April 2010.

1. Phillips, M. M. *et al.* The reddening-free decline rate versus luminosity relationship for Type IA supernovae. *Astron. J.* **118,** 1766–1776 (1999).
2. Permutter, S. *et al.* Measurements of Ω and Λ from 42 high-redshift supernovae. *Astrophys. J.* **517,** 565–586 (1999).
3. Riess, A. *et al.* Observational evidence from supernovae for an accelerating universe and a cosmological constant. *Astron. J.* **116,** 1009–1038 (1998).
4. Kuhlen, M., Woosley, S. E. & Glatzmaier, G. A. Carbon ignition in type Ia supernovae. II. A three-dimensional numerical model. *Astrophys. J.* **640,** 407–416 (2006).
5. Kasen, D., Röpke, F. K. & Woosley, S. E. The diversity of type Ia supernovae from broken symmetries. *Nature* **460,** 869–872 (2009).
6. Maeda, K. *et al.* Nucleosynthesis in two-dimensional delayed detonation models of type Ia supernova explosions. *Astrophys. J.* **712,** 624–638 (2010).
7. Röpke, F. K., Woosley, S. E. & Hillebrandt, W. Off-center ignition in type Ia supernovae. I. Initial evolution and implications for delayed detonation. *Astrophys. J.* **660,** 1344–1356 (2007).
8. Jordan, G. C. *et al.* Three-dimensional simulations of the deflagration phase of the gravitationally confined detonation model of type Ia supernovae. *Astrophys. J.* **681,** 1448–1457 (2008).
9. Branch, D., Drucker, W. & Jeffery, D. J. Differences among expansion velocities of type Ia supernovae. *Astrophys. J.* **330,** L117–L118 (1988).
10. Benetti, S. *et al.* The diversity of type Ia supernovae: evidence for systematics? *Astrophys. J.* **623,** 1011–1016 (2005).
11. Khokhlov, A. M. Delayed detonation model for type Ia supernovae. *Astron. Astrophys.* **245,** 114–128 (1991).
12. Iwamoto, K. *et al.* Nucleosynthesis in Chandrasekhar mass models for type Ia supernovae and constraints on progenitor systems and burning-front propagation. *Astrophys. J.* **125** (Suppl.), 439–462 (1999).
13. Nomoto, K., Thielemann, F.-K. & Yokoi, K. Accreting white dwarf models of type I supernovae. III – carbon deflagration supernovae. *Astrophys. J.* **286,** 644–658 (1984).
14. Woosley, S. E. & Weaver, T. A. The physics of supernova explosions. *Annu. Rev. Astron. Astrophys.* **24,** 205–253 (1986).
15. Höflich, P. *et al.* Maximum brightness and postmaximum decline of light curves of type Ia supernovae: a comparison of theory and observations. *Astrophys. J.* **472,** L81–L84 (1996).
16. Mazzali, P. A., Röpke, F. K., Benetti, S. & Hillebrandt, W. A common explosion mechanism for type Ia supernovae. *Science* **315,** 825–828 (2007).
17. Benetti, S. *et al.* Supernova 2002bo: inadequacy of the single parameter description. *Mon. Not. R. Astron. Soc.* **348,** 261–278 (2004).
18. Branch, D., Fisher, A. & Nugent, P. On the relative frequencies of spectroscopically normal and peculiar type Ia supernovae. *Astron. J.* **106,** 2383–2391 (1993).
19. Maeda, K. *et al.* Nebular spectra and explosion asymmetry of type Ia supernovae. *Astrophys. J.* **708,** 1703–1715 (2010).
20. Fink, M. *et al.* Double-detonation sub-Chandrasekhar supernovae: can minimum helium shell masses detonate the core? *Astron. Astrophys.* (submitted); preprint at ⟨http://arXiv.org/abs/1002.2173⟩ (2010).
21. Stehle, M., Mazzali, P. A., Benetti, S. & Hillebrandt, W. Abundance stratification in type Ia supernovae – I. The case for SN 2002bo. *Mon. Not. R. Astron. Soc.* **360,** 1231–1243 (2005).
22. Wang, L., Baade, D. & Patat, F. Spectropolarimetric diagnostics of thermonuclear supernova explosions. *Science* **315,** 212–214 (2007).
23. Neill, J. D. *et al.* The local hosts of type Ia supernovae. *Astrophys. J.* **707,** 1449–1465 (2009).
24. Jha, S. *et al.* The type Ia supernova 1998bu in M96 and the Hubble constant. *Astrophys. J.* **125** (Suppl.), 73–97 (1999).
25. Cappellaro, E. *et al.* Detection of a light echo from SN 1998bu. *Astrophys. J.* **549,** L215–L218 (2001).
26. Filippenko, A. V. *et al.* The subluminous, spectroscopically peculiar type Ia supernova 1991bg in the elliptical galaxy NGC 4374. *Astron. J.* **104,** 1543–1556 (1992).
27. Turatto, M. *et al.* The properties of the peculiar type Ia supernova 1991bg. I. Analysis and discussion of two years of observations. *Mon. Not. R. Astron. Soc.* **283,** 1–17 (1996).
28. Morrell, N., Folatelli, G. & Stritzinger, M. Supernova 2007on in NGC 1404. *Cent. Bur. Electron. Telegr.* **1131** (2007).
29. Altavilla, G. *et al.* The early spectral evolution of SN 2004dt. *Astron. Astrophys.* **475,** 585–595 (2007).
30. Wang, X. *et al.* Improved distances to type Ia supernovae with two spectroscopic subclasses. *Astrophys. J.* **699,** L139–L143 (2009).

Supplementary Information is linked to the online version of the paper at www.nature.com/nature.

Acknowledgements We thank W. Hillebrandt for discussions. This study is partly based on observations obtained at the Gemini Observatory, Chile (GS-2009B-Q-8, GS-2008B-Q-32/40/46), the Magellan Telescopes, Chile, and by ESO Telescopes at the La Silla or Paranal Observatories under programme 080.A-0516. This research made use of the SUSPECT archive, at the Department of Physics and Astronomy, University of Oklahoma. This work was supported by World Premier International Research Center Initiative (WPI Initiative), MEXT, Japan. K.M. was supported by a JSPS Grant-in-Aid for young scientists; S.B. acknowledges partial support from ASI contracts 'COFIS'; M.S. was supported by the National Science Foundation; F.K.R. was supported through the Emmy Noether Program of the German Research Foundation and by the Cluster of Excellence 'Origin and Structure of the Universe'; G.F. and M.H. acknowledge support from Iniciativa Cientifica Milenio and CONICYT programmes FONDECYT/FONDAP/BASAL; J.S. is a Royal Swedish Academy of Sciences Research Fellow supported by the Knut and Alice Wallenberg Foundation; and S.T. acknowledges support from the Transregional Collaborative Research Centre under the programme 'The dark Universe'. The Dark Cosmology Centre is funded by the Danish National Research Foundation.

Author Contributions S.B. and K.M. found the relation between the velocity gradient and the nebular velocity, and initiated and organized the project. K.M. wrote the manuscript with the assistance of M.S., J.S., G.F. and S.T. S.B. is responsible for the late-phase spectrum of SN 1997bp. M.S., G.F. and M.H are responsible for acquisition and reduction of SN 2007on, SN 2007sr and SN 2009ab. F.K.R. and K.M. are responsible for the explosion simulation. All the authors contributed to discussions.

Author Information Reprints and permissions information is available at www.nature.com/reprints. The authors declare no competing financial interests. Readers are welcome to comment on the online version of this article at www.nature.com/nature. Correspondence and requests for materials should be addressed to K.M. (keiichi.maeda@ipmu.jp).